ND_3-density distribution in orientationally disordered $Ni(ND_3)_6Cl_2$ observed by means of neutron Laue diffraction

2000 J. Phys.: Condens. Matter 12 8567

(http://iopscience.iop.org/0953-8984/12/40/302)

J. Phys.: Condens. Matter **12** (2000) 8567–8576. Printed in the UK PII: S0953-8984(00)13005-X

ND_3-density distribution in orientationally disordered $Ni(ND_3)_6Cl_2$ observed by means of neutron Laue diffraction

P Schiebel†, K Burger†, H G Büttner‡, G J Kearley§, M Lehmann‡ and W Prandl†

† Institut für Kristallographie der Universität Tübingen, Charlottenstraße 33, D-72070 Tübingen, Germany

‡ Institut Laue–Langevin, Grenoble, France

§ Interfacultair Reactor Instituut, Technische Universiteit Delft, Delft, The Netherlands

Received 4 April 2000

Abstract. Neutron Laue diffraction combined with the maximum-entropy method yields a powerful tool for direct observation of the density distribution of dynamically disordered molecules. Laue diffraction investigation delivers a systematically incomplete data set in a very much shorter time than using a conventional four-circle diffractometer, and the maximum-entropy method is an easy tool to use to cope with the gaps in the data set. From the calculated proton-density distribution the molecular hindering potential was successfully derived in the case of $Ni(ND_3)_6Cl_2$.

1. Introduction

The direct observation of the nuclear density distribution of disordered molecules is, in principle, a standard crystallographic routine. The scattering density is obtained by calculating Fourier maps from phased neutron data sets obtained from single-crystal diffraction. This classical Fourier technique carries an inherent drawback: the broadening of all details by series termination effects and the failure of the density synthesis for incomplete data sets, in particular when strong Fourier components, i.e. intense Bragg reflections, are missing. The maximum-entropy-method (MEM) reconstruction of the densities is, by virtue of its construction from the principles of probability theory, an attempt to determine the most probable scattering density from an incomplete data set. It is successful in many different applications (for a current review of applications in crystallography, see Gilmore [1]).

In the case of dynamically disordered molecules the observed nuclear density distribution yields a direct image of the nuclear motion or molecular dynamics. Here the MEM yields the high quality in spatial resolution which is necessary [2–4], since an accurate density distribution is the basic requirement for the determination of the hindering potential in orientationally disordered molecular crystals [5, 6].

In this paper we report a new method for determining the hindering potential experienced by the dynamically disordered NH_3 molecules in $Ni(NH_3)_6Cl_2$: we use the very fast data collection available by means of neutron Laue diffraction using an image plate, and combine it with the ability of the MEM to cope with the unavoidable gaps in the data set. The MEM proton density obtained is then used to calculate the hindering potentials. In contrast to data sets observed using a four-circle diffractometer, data sets obtained from Laue diffraction in general yield an incomplete set of Bragg reflections because the wavelength distribution leads to

0953-8984/00/408567+10$30.00

multiple coincidences of reflections (h, k, l) with their corresponding higher-order reflections (nh, nk, nl). However, Laue diffraction investigation has the advantage of delivering a data set in a time which is an order of magnitude smaller.

This paper is organized as follows. In section 2 the basic features of the NH_3 orientational disorder in metal hexa-ammine salts are summarized. The sample preparation and experimental set-up are described in section 3, and the results of the structural analysis in section 4. Section 5 shows the maximum-entropy reconstruction of the proton-density distribution. The analysis of this density and a comparison of the new results with previous results obtained from other metal hexa-ammine compounds is given in section 6.

2. Dynamical disorder in $M(NX_3)_6Y_2$ compounds

Compounds of the family $M(NX_3)_6Y_2$ with M = Ni, Co; X = H, D; Y = Br, Cl, I, NO_3, PF_6 are isomorphous. In their high-temperature phase they generally form a face-centred-cubic lattice (space group: $Fm\bar{3}m$), where the basic unit is a cube of Y ions which surround one $M(NX_3)_6$ octahedron [5, 7] (figure 1). The incompatibility of the molecular symmetry $3m$ of NX_3 with the symmetry $4mm$ of the lattice site gives rise to the orientational disorder found in these compounds (figure 1(b)). On cooling, various phase transitions are observed and it was suggested that they are triggered by the freezing of NH_3 groups [8, 9].

While for the low-temperature phases a detailed crystallographic description is still lacking, in the high-temperature phases the orientations of the ammine groups are usually described in terms of dynamical disorder between a number of different sites.

In recent studies on a series of nickel and cobalt hexa-ammine compounds in their cubic phases [5, 6], we obtained the scattering densities from the orientationally disordered protons and deuterons by Fourier and MEM techniques and observed a nuclear density distribution with four maxima at the corners of a square for the compounds with Y = Br, I, NO_3 (figure 2), whereas a nearly circular density distribution was found for Y = PF_6. All observed density distributions could consistently be explained as the consequence of rotation–translation coupling in an anharmonic crystal potential. The centre of mass of the ammonia group performs an anticlockwise rotation around the fourfold crystal axis, while the molecule rotates clockwise around its threefold axis [5, 10].

Within the model of rotation–translation coupling, the dynamical problem of the ammonia motion is reduced to the motion of a rigid H/D_3 triangle in a plane perpendicular to the Ni–N axis, where the observed proton density is concentrated. This motion is determined by the time-independent two-dimensional anharmonic mean crystal potential V_{Cr}, which is expanded into symmetry-adapted functions, according to the local site symmetry $4mm$:

$$V_{Cr}(r, \phi) = \frac{1}{2}Ar^2 + \frac{1}{4}Br^4 \cos 4\phi + \frac{1}{4}Cr^4 \tag{1}$$

where (r, ϕ) is the position of one H atom. This anharmonic potential couples the rotational motion of the H_3 triangle to its centre-of-mass motion. The parameter A denotes the strength of the coupling whereas B and C measure the anharmonicity of the potential.

The effective molecular potential for one setting of the H_3 triangle is given by the sum of the single-particle potentials of each of the three protons:

$$V_M(R_c, \phi_c, \beta) = \sum_{p=0}^{2} V_{Cr}(r_p, \phi_p). \tag{2}$$

The Boltzmann probability for one configuration (R_c, ϕ_c, β) is known to be

$$\rho(R_c, \phi_c, \beta) = Z^{-1} \mathrm{e}^{-V_M(R_c, \phi_c, \beta)/kT} \tag{3}$$

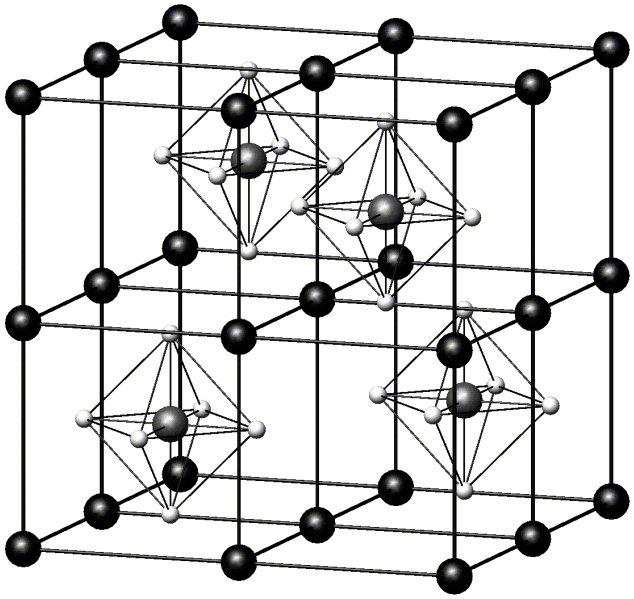

(a)

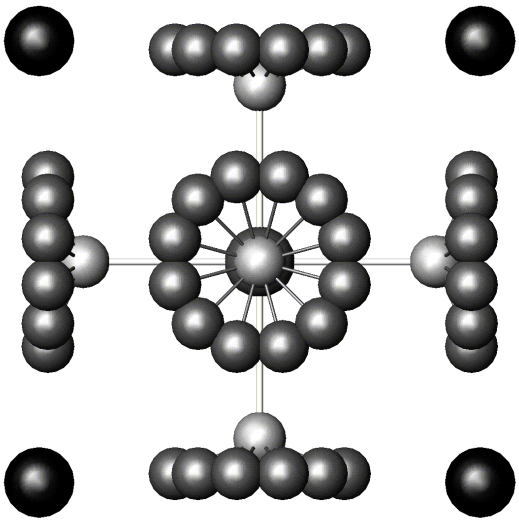

(b)

Figure 1. (a) The crystal structure ($Fm3m$) of $M(NH_3)_6Y_2$, M = Ni, Co, ...; Y = Br, Cl, I, ... The face-centred-cubic structure is built from Y cubes (black), where every second cube is occupied by a $M(NH_3)_6$ octahedron. Hydrogen atoms are not shown. (b) Projection of one $M(NH_3)_6$ octahedron with its surrounding Y cube. According to the local symmetry $4mm$, the ammonia molecules are shown in four split positions, leading to twelve hydrogen positions for each ammonia molecule.

where Z is the partition function. From this the scattering length density, $\rho(x, y)$ is obtained by taking a configurational average:

$$\rho(x, y) = 3Z^{-1}\mathrm{e}^{-V^0_{Cr}(x,y)/kT} \int \mathrm{e}^{-(V^1_{Cr}+V^2_{Cr})/kT}\,\mathrm{d}\gamma. \tag{4}$$

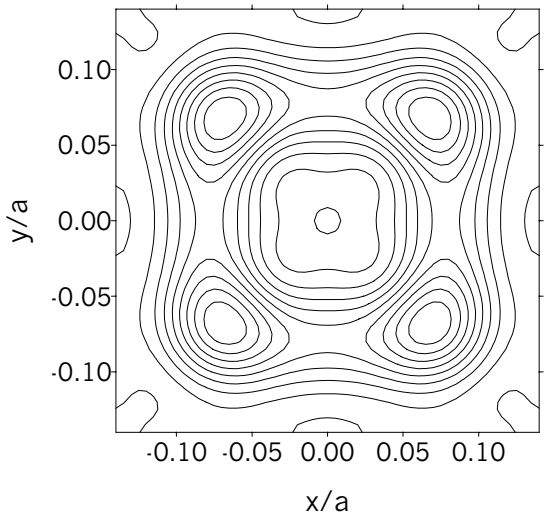

Figure 2. The Fourier density of $Ni(ND_3)_6Br_2$ obtained from a neutron single-crystal experiment on a four-circle diffractometer [5]. The cut is at $z = z_D = 0.24$ where the maximum deuteron density occurs.

Thus the mean crystal potential may be determined by a least-squares analysis of the observed densities [5, 6].

3. Neutron Laue diffraction

Single crystals were synthesized from aqueous solution. Deuterated samples were prepared by dissolving $Ni(NO_3)_2{\cdot}6D_2O$ in a concentrated deuterated ammonia solution to give $Ni(ND_3)_6(OD)_2$. Adding ND_4Cl and heating to 70 °C yielded an oversaturated solution. On cooling down to room temperature, single crystals with blue colour and octahedral shape grew.

In the Laue-diffraction experiment we used a small single crystal of deuterated nickel hexaammine chloride, $Ni(ND_3)_6Cl_2$. The blue, octahedral crystal had a volume of only 1.5 mm^3. We measured four neutron Laue diagrams at room temperature with different crystal settings ($\phi = 0°, 20°, 40°, 60°$), for 50 min each. Upon indexing and integrating the measured data, 105 symmetry-independent single Bragg reflections were obtained (94 with $F > 4\sigma_F$). In the indexing routine we used the lattice parameter $a = 10.06(1)$ Å, which we had determined by means of x-ray powder diffraction. The absorption correction was found to be negligible. The extinction correction was included in the structure refinement [11]. Details are given in table 1.

4. Structure refinement

The main purpose of the structure refinement with split-atom or split-molecule models is to determine a set of signs for the measured $|F^{obs}_{hkl}| \sim \sqrt{I^{obs}_{hkl}}$ which is independent of details of the specific model. These signed F_{hkl} are then used to extract the deuteron density via Fourier techniques or MEM reconstruction. For the structure refinement we used SHELXL97 [11]. The refinement of the ammonia hydrogens follows the approach shown in [6, 10].

The rigid ammonia molecule is treated in three different split-molecule settings. For two settings the molecular mirror plane coincides with one of the two mirror planes of the local site symmetry $4mm$. The third model consists of a molecule in a general position, which leads to twelve H positions around the fourfold crystal axis. Within this model, refinement of anisotropic thermal parameters turned out to be unstable. The model leading to the smallest

Table 1. Experimental details.

Crystal data	
Chemical formula	$Ni(NH_3)_6Cl_2$
Chemical formula weight	249.60
Crystal shape	Octahedral
Crystal colour	Blue
Sample volume	1.5 mm^3
Temperature	295 K
Cubic space group	$Fm\bar{3}m$
Lattice constant a	10.06(1) Å
Cell volume V	1018.1(18) $Å^3$
Z	4
D_x	1.623 Mg m^{-3}
Data collection	
Neutrons	
Laue diffractometer at ILL	
White beam: 1.0 to 1.83 $Å^{-1}$	
945 measured reflections	
105 independent reflections	
94 reflections with $I > 2\sigma(I)$	
$R_{int} = 0.0381$	

R-values is given in table 2. There were no significant differences among the Ni, N, Cl parameters refined with the different models. The Ni–N bond distance is $d_{Ni-N} = 2.130(4)$ Å, in agreement with the distances found in [5].

The different models for the deuterium positions reveal that the density is concentrated on a plane which is perpendicular to the respective Ni–N axis. The centre of mass of the deuterium triangle coincides with the fourfold crystal axis; therefore the tilt angle is negligible.

However, our goal was to determine the phases of the measured $|F_{hkl}|$. The decisive point is that as soon as hydrogens are included in the refinement there are no longer any differences among the phases of the structure factors calculated with the different models, i.e. they are independent with respect to the refined parameters. In this way we obtained a unique, model-independent set of phases for the observed structure factors.

5. Nuclear density distribution

From the measured structure factors, together with the stable, 'model-independent' phases, one may expect to obtain a 'model-free' observed scattering density, provided that the linear inverse Fourier transform can be handled satisfactorily. For comparison, we calculated the scattering density by standard Fourier transformation and by the maximum-entropy-method reconstruction described below. The latter involved a discretization of the unit cell into a $128 \times 128 \times 128$ grid.

Figures 3 and 4 show cuts through the $Ni(ND_3)_6$ octahedron parallel to the face of the unit cube at $z = 0$ and $z = z_D = 0.24$ where the maximum deuteron density occurs.

In the section at $z = 0$ through the scattering length density obtained by Fourier transformation, the central Ni and the surrounding N atoms are clearly visible (figure 3(a)). The Cl ions, located at $z_{Cl} = 0.25$, show up in the corresponding section at $z = z_D = 0.24$, due to their thermal motion (figure 3(b)). However, no deuterium contribution to the scattering

Table 2. Results of the structure refinement with SHELXL97 [11].

Atomic parameters:		x	y	z	Occupancy	U_{eq}	
	Ni	0.0000	0.0000	0.0000	1.00	0.0299(9)	
	N	0.2500	0.2500	0.2500	1.00	0.043(1)	
	Cl	0.2117(3)	0.0000	0.0000	1.00	0.0515(8)	
	D1	0.077(2)	0.064(3)	0.241(2)	0.25	0.074(4)	
	D2	0.0000	−0.074(3)	0.239(4)	0.25	0.11(2)	
Anisotropic thermal parameters:		u_{11}	u_{22}	u_{33}	u_{23}	u_{13}	u_{12}
	N	0.036(2)	0.059(2)	0.059(2)	0.000	0.000	0.000
	D1	0.045(5)	0.13(2)	0.052(3)	−0.010(9)	−0.011(5)	−0.011(4)
	D2	0.20(7)	0.07(1)	0.07(1)	0.01(1)	0.000	0.000

Refinement on F^2

$R_{all} = 0.0916$

$R[F^2 > 2\sigma(F^2)] = 0.0622$

$wR(F^2) = 0.0776$

$wR_{obs} = 0.0736$

$S = 1.438$

Restrained $S = 1.444$

105 reflections

24 parameters

5 restraints

Weighting scheme:

$w = 1/[\sigma^2 F_o^2 + (0.0060P)^2 + 5.7676P]$

where $P = (F_o^2 + 2F_c^2)/3$

Extinction correction:

$F_c^* = kF_c[1 + 0.001\chi F_c^2 \lambda^3 / \sin(2\theta)]^{-1/4}$

Extinction coefficient $\chi = 0.020(7)$

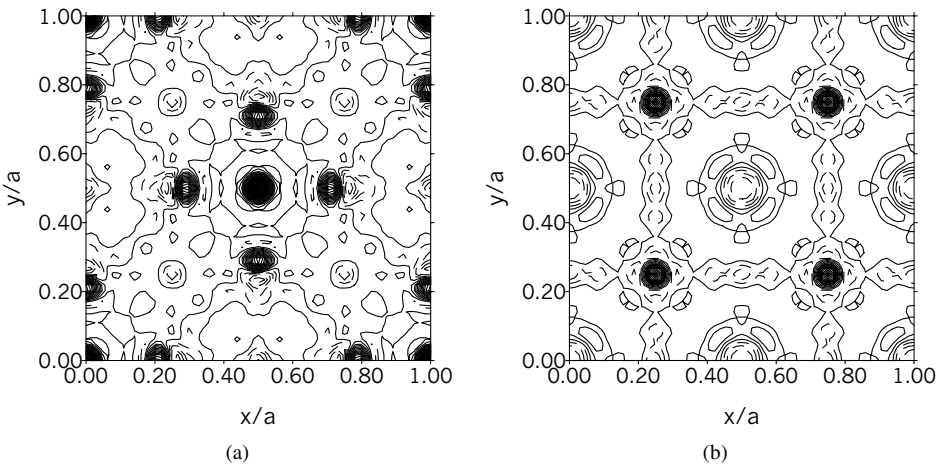

Figure 3. The Fourier density of $Ni(ND_3)_6Cl_2$. (a) A cut at $z = 0$. (b) A cut at $z = z_D = 0.24$ where the maximum deuteron density occurs.

length density is found. The Fourier densities suffer from severe truncation errors and the residual noise, which leads to spurious density between the atomic positions.

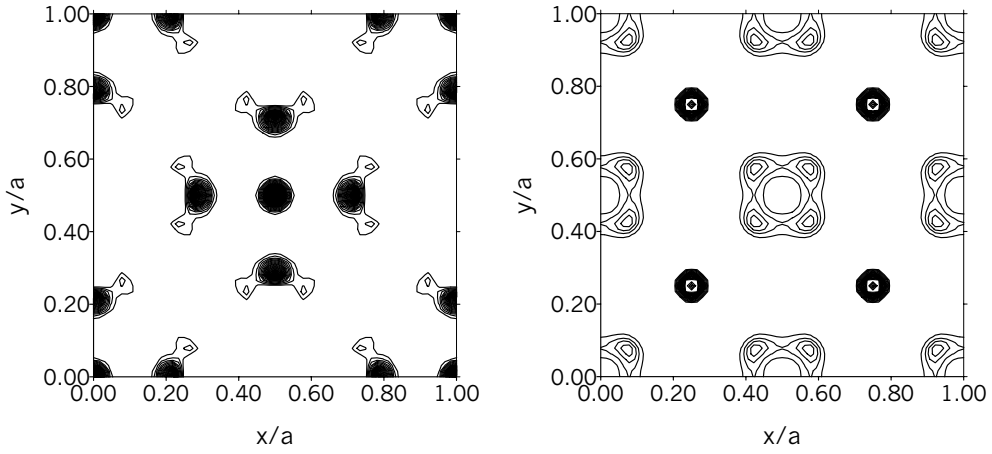

Figure 4. A maximum-entropy reconstruction of the density of $Ni(ND_3)_6Cl_2$. (a) A cut at $z = 0$. (b) A cut at $z = z_D = 0.24$ where the maximum deuteron density occurs.

In contrast, the density reconstructed by the MEM from the same input data clearly shows the deuterium contribution to the scattering length density (figure 4).

The deuteron density obtained in $Ni(ND_3)_6Cl_2$ is concentrated on a plane perpendicular to the fourfold crystal axis. The density in this plane shows four maxima on a square (figure 4(b)). The distances between these maxima do not correspond to the ammonia D–D distance. In addition, the distance to the fourfold crystal axis is larger than the rotational radius of an ammonia group. This finding can only be explained by a movement of the ammonia centre of mass combined with the rotational motion of the ammonia molecule, and is due to the rotational–translational coupling found in these compounds [5].

5.1. The maximum-entropy method (MEM)

The non-linear MEM, which has its roots in probability and information theory, has been applied to many fields of crystallography (Gilmore [1]). Such work includes: the attempt to observe the binding electron density between Si atoms directly (Sakata and Sato [12]; Takata and Sakata [13]); application to powder data sets with overlapping reflections (Sakata, Mori, Kumazawa, Takata and Toraya [14]); application to neutron data, where negative scattering densities can occur (Takata, Sakata, Kumazawa, Larsen and Iversen [15]); investigation of disordered structures (Papoular, Prandl and Schiebel [16]); polarized neutron scattering studies (Papoular, Zheludev, Ressouche and Schweizer [17]; Schleger, Puig-Molina, Ressouche, Rutty and Schweizer [18]); extraction of strictly positive integrated intensities from strongly overlapping powder reflections (Sivia and David [19]); investigation of quasicrystals (Haibach and Steurer [20]); investigation of single-crystal Laue data sets (Bourenkov, Popov and Bartunik [21]); phase determination by statistical (direct) methods (Bricogne and Gilmore [22]).

The MEM algorithm is an attempt to calculate the most probable density distribution with the data given. In the case of x-ray data it incorporates the physical knowledge that the scattering density has to be strictly positive. In the case of incomplete data sets, we usually found it to give much better results than the simple linear Fourier transformation, where the unavoidable gaps in the data set often lead to severe disturbances of the Fourier density calculated. Also, the

estimated errors of observations are taken into account in the calculation. A disadvantage of the current simple algorithm is that the MEM density calculated is not completely quantitative, but more a qualitative density distribution: especially when high-order reflections are missing, the MEM-density distribution of a single atom or nucleus sometimes appears to be 'sharpened' or 'too peaky'.

Although the current MEM algorithms are far from being perfect (see e.g. Brummerstedt-Iversen, Jensen and Danielsen [23] and references therein), the MEM has been shown to be well suited for incomplete anomalous dispersion x-ray powder data sets: with the MEM all the different types of information obtained there (from phased and unphased, unique and overlapping reflections) can be used together in one calculation of the electron-density distribution (Burger, Prandl and Doyle [24]; Burger [25]; Burger and Prandl [26]). The MEM program that we used is written in FORTRAN77 and can be obtained from Internet address http://www.uni-tuebingen.de/uni/pki without charge. It is described in detail by Burger [27] and is essentially an enhanced version of the original Japanese program MEED (Kumazawa, Kubota, Takata and Sakata [28]) (see the Internet address http://www.mcr.nuap.nagoya-u.ac.jp/mem).

6. Results and discussion

The density distribution found in the present Laue-diffraction study for $Ni(ND_3)_6Cl_2$ is very similar to the density distribution observed in $Ni(ND_3)_6Br_2$ (figure 2). It also shows four maxima at the corners of a square. This clearly indicates the importance of rotation–translation coupling in these compounds.

Therefore we used the central part of the two-dimensional map given in figure 4(b) as input data for a refinement of the potential parameters A, B, C (1). In addition, a scale factor s and the distance d_p of the three protons from their centre of mass were refined. The refinement converged rapidly. The refined parameters are $A = -554.070(3)$ K Å^{-2}, $B = 432.25(2)$ K Å^{-4}, $C = 1432.56(8)$ K Å^{-4}, $d_p = 0.9620(3)$ Å. For comparison with our previous results, derived from neutron single-crystal data recorded on a four-circle diffractometer, figure 5 shows the potential parameters versus the anion radius. The new

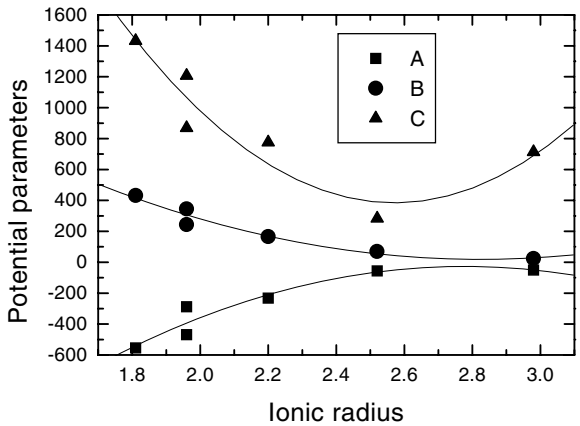

Figure 5. Potential parameters A, B, C of the mean crystal potential $V_{Cr}(r, \phi) = \frac{1}{2}Ar^2 + \frac{1}{4}Br^4 \cos 4\phi + \frac{1}{4}Cr^4$ (equation (1)) versus the ionic radius for a series of metal hexa-ammine compounds. ($[A]$ = K Å^{-2}, $[B]$ = K Å^{-4}, $[C]$ = K Å^{-4}.)

parameter set fits perfectly into the series of parameters obtained previously by Fourier techniques applied to data sets obtained with a four-circle diffractometer.

In passing, we want to emphasize another aspect, namely the different amounts of beam time required to collect these data sets. On average six days were required to make the measurements for one single crystal of 30 mm^3 volume on a four-circle diffractometer, whereas we measured four sets at different orientations, for 50 minutes each, with a small single crystal of only 2 mm^3 volume. Thus more than a factor of 100 is gained by using Laue diffraction and the MEM together.

Our ultimate goal is to interpret the disordered proton density using a thermodynamic model. Measurements at different temperatures will allow us to determine the temperature dependence of the orientational potential and thus provide an understanding of the order–disorder phase transitions. In addition, using this technique the transition from classical motion to quantum behaviour may be studied.

Neutron Laue diffraction combined with maximum-entropy methods yields a powerful and effective tool for a direct observation of the density distribution of dynamically disordered molecules. It offers a new and unique method for studying the freezing of molecules in crystals and the associated order–disorder phase transitions.

Acknowledgments

This investigation was supported in part by the EU-TMR, DFG and BMBF.

References

[1] Gilmore C J 1996 *Acta Crystallogr.* A **52** 561
[2] Papoular R J, Prandl W and Schiebel P 1992 *Maximum Entropy and Bayesian Methods (Seattle, 1991)* ed C R Smith *et al* (Dordrecht: Kluwer Academic) pp 359–76
[3] Papoular R J, Cousson A, Paulus W and Kaiser-Morris E 1997 *Physica* B **234–236** 72
[4] Schiebel P *et al* 1999 *Phys. Rev. Lett.* **83** 975
[5] Schiebel P *et al* 1995 *J. Phys.: Condens. Matter* **6** 10 989
[6] Schiebel P, Prandl W, Papoular R and Paulus W 1996 *Acta Crystallogr.* A **52** 189
[7] Wyckoff R W G (ed) 1965 *Crystal Structures* vol 3 (New York: Wiley–Interscience) p 783
[8] Bates A R and Stevens K W H 1969 *J. Phys. C: Solid State Phys.* **2** 1573
[9] Eckert J and Press W 1980 *J. Chem. Phys.* **73** 451
[10] Schiebel P, Hoser A, Prandl W and Heger G 1990 *Z. Phys.* B **81** 253
[11] Sheldrick G M 1997 *SHELXL97. Program for the Refinement of Crystal Structures* University of Göttingen, Germany
[12] Sakata M and Sato M 1990 *Acta Crystallogr.* A **46** 263
[13] Takata M and Sakata M 1996 *Acta Crystallogr.* A **52** 287
[14] Sakata M *et al* 1990 *J. Appl. Crystallogr.* **23** 526
[15] Takata M *et al* 1994 *Acta Crystallogr.* A **50** 330
[16] Papoular R, Prandl W and Schiebel P 1992 *Maximum Entropy and Bayesian Methods* (Kluwer: Dordrecht)
[17] Papoular R, Zheludev A, Ressouche E and Schweizer J 1995 *Acta Crystallogr.* A **51** 295
[18] Schleger P *et al* 1997 *Acta Crystallogr.* A **53** 426
[19] Sivia D and David W 1994 *Acta Crystallogr.* A **50** 703
[20] Haibach T and Steurer W 1995 *Acta Crystallogr.* A **52** 277
[21] Bourenkov G, Popov A and Bartunik H 1996 *Acta Crystallogr.* A **52** 797
[22] Bricogne G and Gilmore C 1990 *Acta Crystallogr.* A **46** 284
[23] Brummerstedt-Iversen B, Jensen J L and Danielsen J 1997 *Acta Crystallogr.* A **53** 376
[24] Burger K, Prandl W and Doyle S 1997 *Z. Kristall.* **212** 493
[25] Burger K 1997 Neue Möglichkeiten der Kristallstrukturbestimmung aus Pulverdaten durch die Nutzung resonanter Streuung von Röntgenstrahlung und der 'Maximum-Entropy' Methode *Doktorarbeit* Universität Tübingen (Aachen: Shaker)

[26] Burger K and Prandl W 1999 *Acta Crystallogr.* A **55** 719
[27] Burger K 1998 *Powder Diffract.* **13/2** 117
[28] Kumazawa S, Kubota Y, Takata M and Sakata M 1993 *J. Appl. Crystallogr.* **26** 453